

## Supporting Information

### Probing the Active Site in Single-atom Oxygen Reduction Catalysts via Operando X-ray and Electrochemical Spectroscopy

Hsiang-Ting Lien,<sup>a,b,§</sup> Sun-Tang Chang,<sup>c,§</sup> Po-Tuan Chen,<sup>a,b,d,§</sup> Deniz P. Wong,<sup>e</sup>  
Yu-Chung Chang,<sup>a,c,f</sup> Ying-Rei Lu,<sup>f,g</sup> Chung-Li Dong,<sup>g</sup> Chen-Hao Wang,<sup>c</sup>  
Kuei-Hsien Chen,<sup>a,e\*</sup> and Li-Chyong Chen<sup>a,b\*</sup>

<sup>§</sup> H. T. Lien, S. T. Chang and P. T. Chen contributed equally to this work

<sup>a</sup> Center for Condensed Matter Sciences, National Taiwan University, Taipei, Taiwan

<sup>b</sup> Center of Atomic Initiative for New Materials, National Taiwan University, Taipei, Taiwan

<sup>c</sup> Department of Materials Science and Engineering, National Taiwan University of Science and Technology, Taipei, Taiwan

<sup>d</sup> Department of Vehicle Engineering, National Taipei University of Technology, Taipei, Taiwan

<sup>e</sup> Institute of Atomic and Molecular Sciences, Academia Sinica, Taipei, Taiwan

<sup>f</sup> National Synchrotron Radiation Research Center, Hsinchu, Taiwan

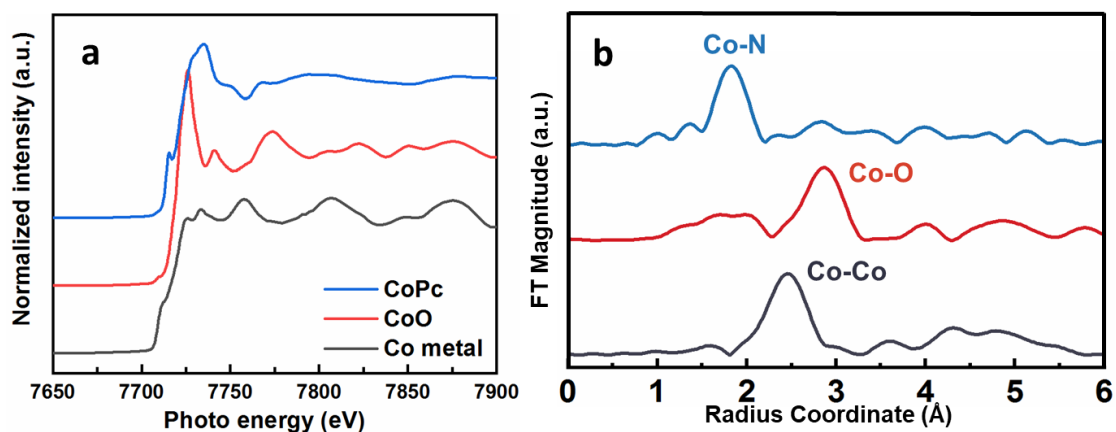
<sup>g</sup> Department of Physics, Tamkang University, Tamsui, Taiwan

\*Corresponding authors:

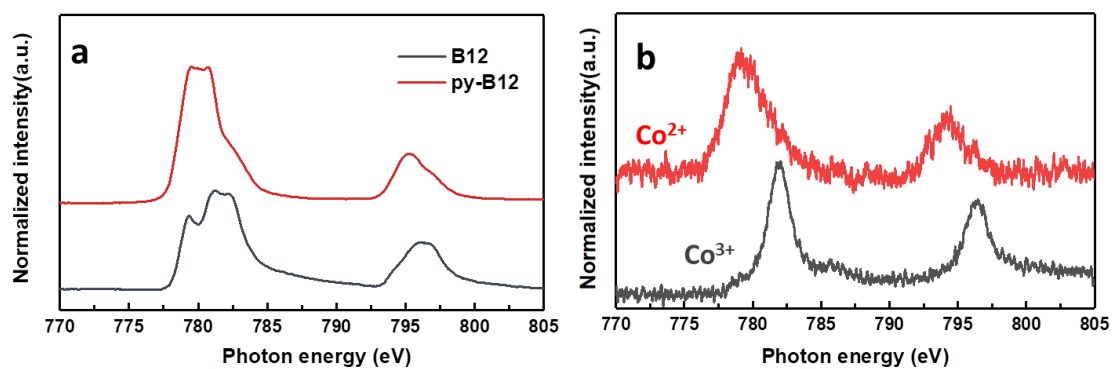
Dr. Li-Chyong Chen: chenlc@ntu.edu.tw

Dr. Kuei-Hsien Chen: chenkh@pub.iam.ssinica.edu.tw

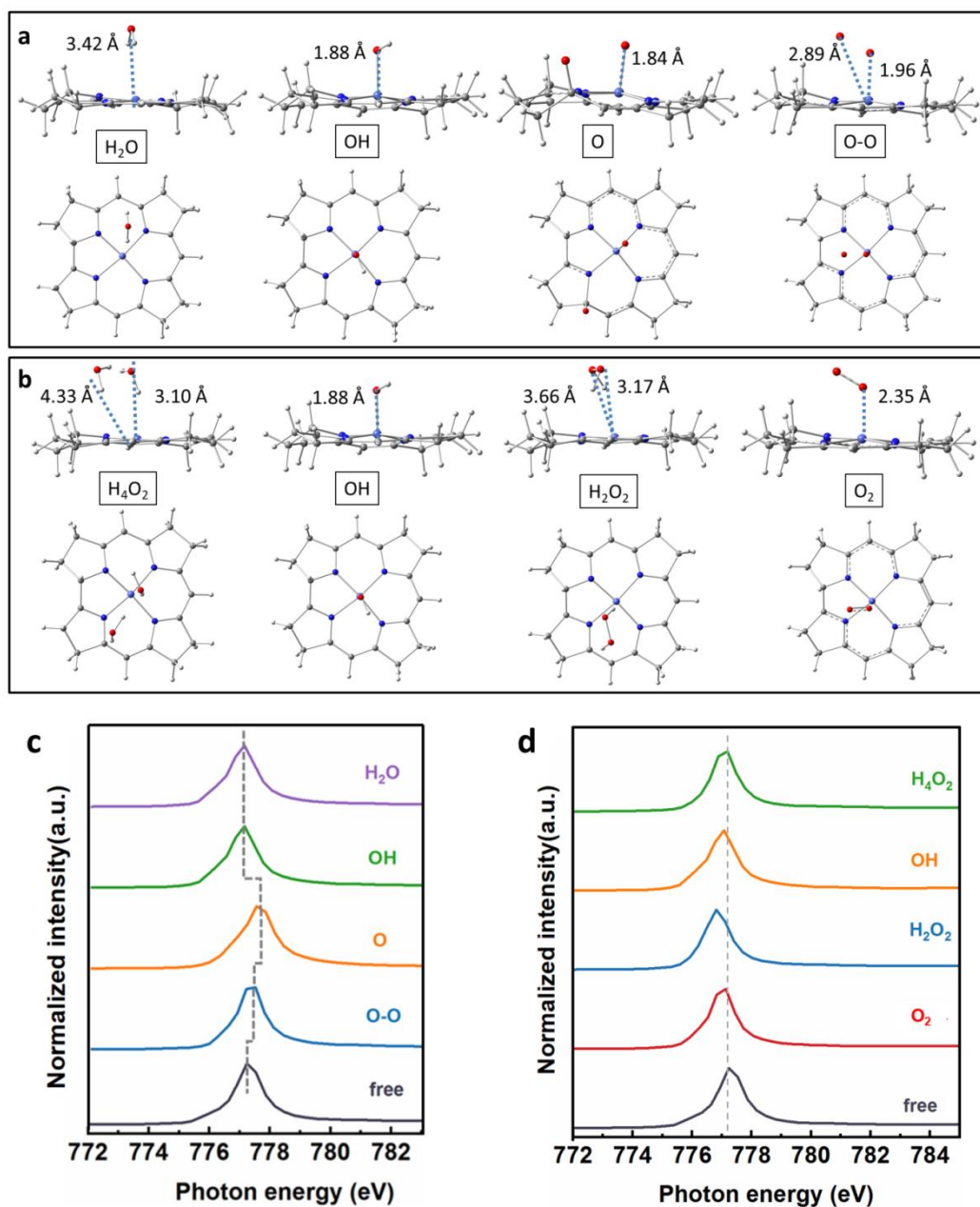
## Supplementary Figures



**Supplementary Figure 1. Ex situ Co K edge XANES and EXAFS spectrum.** (a) Co K edge XANES spectra of three different references, specifically CoPc, CoO and Co metal. (b) The corresponding phase-corrected Fourier transforms EXAFS ( $k^3$ -weighted) from (a).

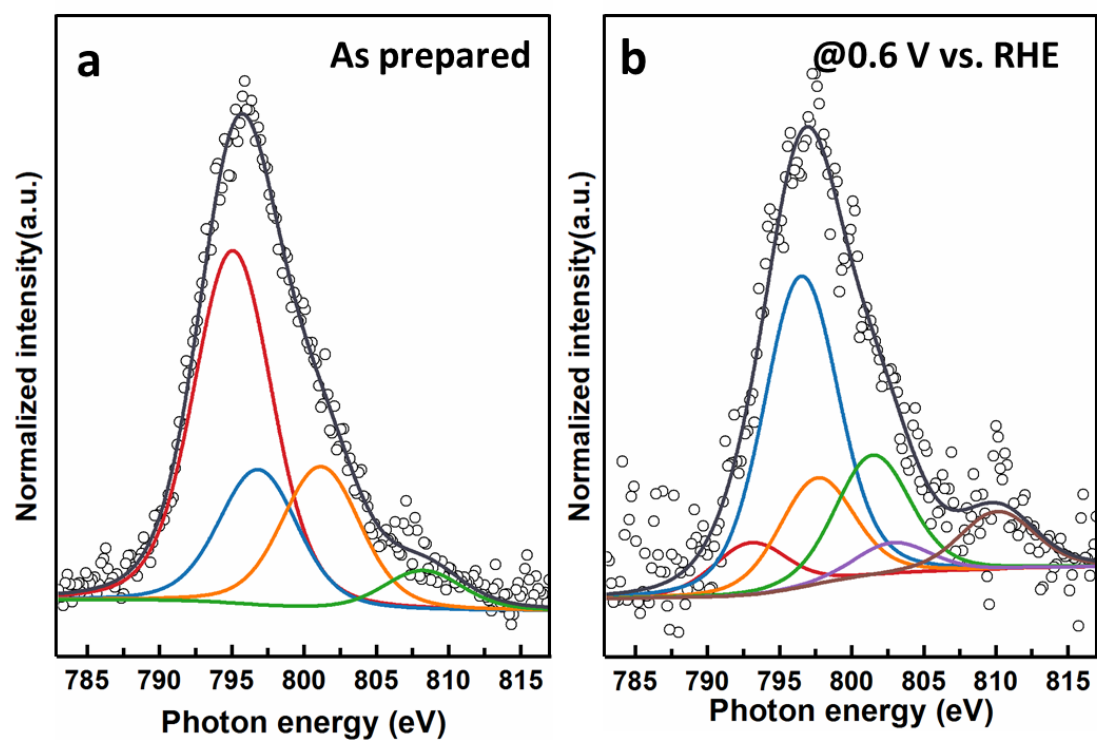


**Supplementary Figure 2. Ex situ Co L edge NEXAFS spectrum.** Soft X-ray absorption Co L<sub>3/2</sub> edge spectra of py-B12 and pristine B12, exhibiting Co<sup>2+</sup> and Co<sup>3+</sup>, respectively. The signals were collected from different mode. (a) Total electron yield (TEY). (b) Total fluorescence yield (TFY).

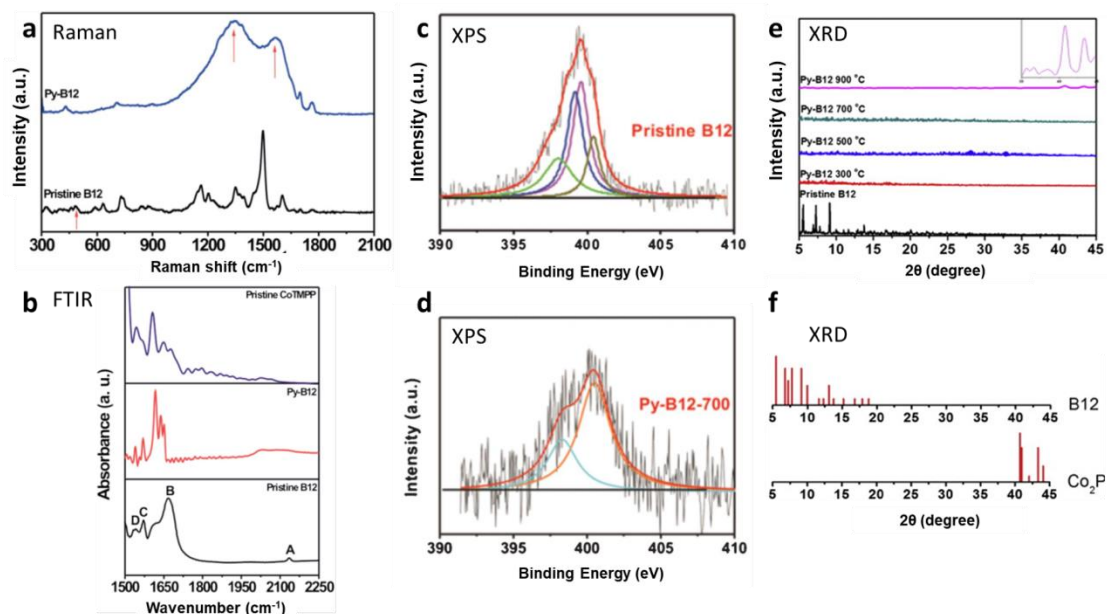


**Supplementary Figure 3. Molecular Orbital Simulation and Co L<sub>3</sub> edge simulated spectrum.** (a) Optimized structures for the models of four-electron process (OO, O, OH, and H<sub>2</sub>O). (b) FEFF calculated Co L edge with the different oxygen species of four-electron process. (c) Optimized structures for the models of two-electron process (O<sub>2</sub>, H<sub>2</sub>O<sub>2</sub>, OH, and H<sub>4</sub>O<sub>2</sub>). (b) FEFF calculated Co L edge with the different oxygen species of two-electron process. If the reaction went through two-electron process, there would be no redshift in the XANES spectrum. XANES calculations were performed using DFT-optimized structures to theoretically examine Co L-edge XANES spectra related to oxygen-based adsorbates on the Co-corrin cluster. XANES calculations of Co were performed by the FEFF8 code. The

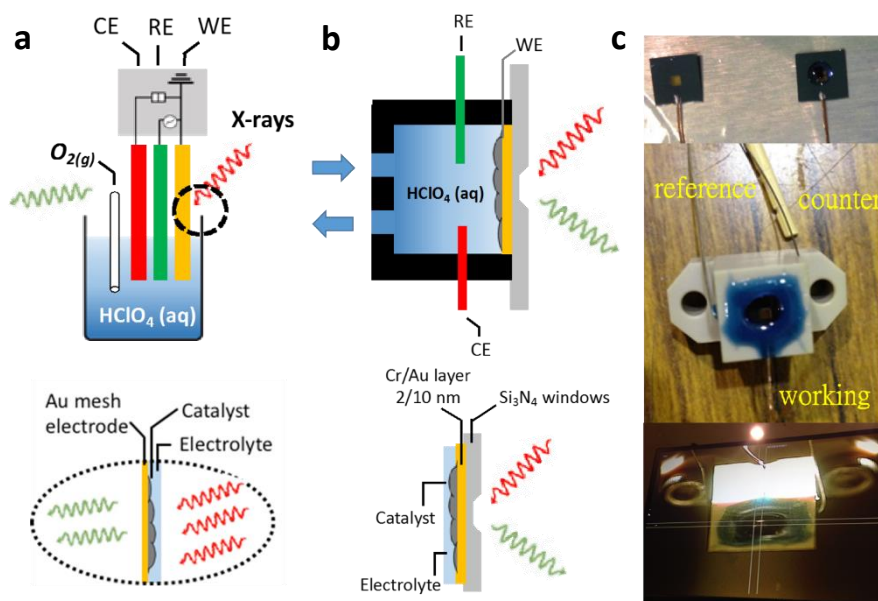
self-consistent potential and full multiple scattering were calculated at a 5.0-Å radius. In the initial input, a negative charge is equally allocated on every atom of a cluster. After self-consistent calculation, the charge would be redistributed correctly. To compare the experimental and calculated spectra, a rigid shift of 2 eV to higher energy was applied to each calculated spectrum.



**Supplementary Figure 4. The Co L<sub>3</sub> edge spectrum fitting.** Soft X-ray absorption of Co L<sub>3</sub> edge spectra of the as prepared py-B12 and under operando potential (@ 0.6V), respectively. The peak fitting results were summarized in **Supplementary Table 2**.



**Supplementary Figure 5. Ex-situ characterizations of electrocatalyst.** (a) Raman of py-B12 and pristine B12 [1], (b) FTIR of py-B12 and pristine B12 [1], (c) XPS of pristine B12 [2], (d) XPS of py-B12 and pristine B12 [2], (e) XRD of py-B12 and pristine B12 [3], and (f) XRD of B12 and Co<sub>2</sub>P [3]. In Raman spectra, the two strong peaks at 1330 and 1580 cm<sup>-1</sup> are attributed to D- and G-peaks, respectively, of the carbon-like materials, suggesting that py-B12 forms a network structure of poly-aromatic hydrocarbons. Similar comparison of the FTIR spectra shows four characteristic peaks (A to D) for pristine B12. XPS suggested that the pyrolysis converts the nitrogen into pyridinic-like nitrogen and quaternary N-type nitrogen, with N<sup>+</sup> at 398.7 eV and 401.4 eV. XRD presented that pristine B12 exhibits the same characteristic peaks as observed in the vitamin B12 reference pattern.



**Supplementary Figure 6. Schematic diagram of in-situ spectroelectrochemical setups.** (a) hard XAS in transmission mode and (b) flow cell for soft XAS in fluorescence mode. (c) Photo for the actual setup used in soft XAS.

## Supplementary Tables

**Supplementary Table 1. The equivalent circuits fitting results.** Analyses of the electrochemical impedance spectra with the respective equivalent circuits proposed in different operation conditions. The fitting elements were assigned to double-layer capacitance of catalyst layer ( $C_{DL}$ ), the charge transfer resistance ( $R_{ct}$ ), mass-transfer resistance ( $R_{mt}$ ) and capacitance of reaction process ( $C_{rxn}$ ). Warburg impedance takes into account a finite diffusion. M is restricted linear ordinary diffusion impedance element with a reflective boundary.

Potential (V vs. RHE)	model	$R_c$ ( $\Omega$ )	$C_{DL}$ (F)	$R_{ct}$ ( $\Omega$ )	$R_{mt}$ ( $\Omega$ )	$C_{rxn}$ (F)	$W(\Omega)$	$M(\Omega)$
1.2 V vs. RHE		16.44	2.82E-3	225.4	--	--	38.05	--
1.0 V vs. RHE		16.44	2.82E-3	222.4	153.7	0.03	--	--
0.8 V vs. RHE		16.44	2.82E-3	124.8	52.05	0.683	--	--
0.6 V vs. RHE		16.44	2.81E-3	68.22	21.6	0.524	--	--
0.4 V vs. RHE		16.44	2.79E-3	44.14	2.65	0.514	--	--
0.2 V vs. RHE		16.44	2.80E-4	30.95	--	--	--	33.39

**Supplementary Table 2. The molecular orbital energy-level diagram.** The  $d^7$  electron  $D_{4h}/S_4$  symmetry crystal field orbital and a hybridization orbital fitting between pre-catalytic and catalytic condition.

Fitting result	As prepared	@ 0.6 V vs. RHE
$d_{x^2-y^2}$	808.22	810.09
$\sigma^* (d_{xy} + \sigma_{2p})$	--	802.81
$\pi_{2p}^*$	--	801.46
$\sigma(d_{xy} + \sigma_{2p})$	--	797.57
$d_{xy}$	801.18	--
$d_{z^2}$	796.84	796.50
$d_{yz}, d_{xz}$	795.09	793.02

## Supplementary References

- [1] Chang, S.-T. et al. Vitalizing fuel cells with vitamins: pyrolyzed vitamin B12 as a non-precious catalyst for enhanced oxygen reduction reaction of polymer electrolyte fuel cells. *Energy Environ. Sci.* **5**, 5305–5314 (2012).
- [2] Wang, C.-H. et al. High stability pyrolyzed vitamin B12 as a non-precious metal catalyst of oxygen reduction reaction in microbial fuel cells. *RSC Adv.* **3**, 15375–15381 (2013).
- [3] Chang, S.-T. et al. Preparation of non-precious metal catalysts for PEMFC cathode from pyrolyzed vitamin B12. *Int. J. Hydrog. Energy* **37**, 13755–13762 (2012).